Zeolite Membranes

DOI: 10.1002/ange.201004029

High-Performance Randomly Oriented Zeolite Membranes Using Brittle Seeds and Rapid Thermal Processing**

*Won Cheol Yoo, Jared A. Stoeger, Pyung-Soo Lee, Michael Tsapatsis, and Andreas Stein**

Intergrown zeolite films prepared by secondary hydrothermal growth of seeded layers are of great interest for size-selective, energy-efficient membrane separations, microelectronic low-dielectric devices, and ion-exchange sensors.[1–3] The task of preparing molecular sieve membranes with high fluxes and separation efficiencies has been addressed through the optimization of growth conditions to obtain preferred crystallographic orientations of zeolite films,[4–6] but this approach usually demands complex procedures. Here, we present a facile method to fabricate MFI zeolite membranes with high flux (ca. 2.6×10^{-7} mol m^{-2} s^{-1} Pa^{-1}) and high separation factors (SF, 123–139 and in one case as high as 335) for xylene isomer separation by optimizing seed deposition and calcination processes. Zeolite nanoparticles prepared by confined syntheses[7,8] were deposited as randomly oriented seed layers on porous supports by rubbing and leveling methods to obtain thin zeolite films (400–500 nm) after secondary hydrothermal growth. Rapid thermal processing (RTP) was used in a single calcination step that substantially reduced processing times and energy usage and improved the separation efficiency of the membranes.

Since Lai et al. reported a high-performance zeolite membrane in which the preferred *b* orientation of zeolite grains (i.e., the direction of straight channels perpendicular to the plane of the membrane) was obtained through the use of crystal shape-modifying, structure-directing agents (SDAs),[5] significant effort has been expended on fabricating oriented membranes by various approaches.[9–15] Although kinetically favorable orientations (*c*- or *hoh*-oriented MFI type zeolite membranes) can be easily achieved by manipulating the secondary growth crystallization temperature, the performance of the resulting intergrown membranes is poor due to grain boundary defects and microcracks that form during SDA removal by calcination.[16,17] Several methods have been explored to deposit oriented MFI seeds on porous supports and to subsequently grow oriented zeolite films, but none have produced zeolite films with sufficiently high permeation, for example, for xylene isomer separation, to be viable in industrial processes.[9,12,14,15,18,19] In order to improve the efficiency of membranes, it is necessary to prepare thinner membrane layers that permit higher permeate fluxes while limiting the formation of debilitating defects and cracks during calcination to maintain high separation factors. A fundamental understanding of zeolite growth from seed particles and of defect formation during calcination would facilitate fabrication of thinner, more efficient membranes for various applications. The use of nanoparticle seeds (<100 nm) and a small filler layer between seeds during secondary growth could be expected to limit crack propagation. Hedlund et al. reported thin, high-flux, zeolite membranes (ca. 500 nm in thickness), but size-selective properties of these MFI-type membranes were limited and separation factors for xylene isomer separation remained moderate.[20,21]

Recently, Choi et al. demonstrated that grain boundary defects could be eliminated through rapid thermal processing (RTP), a calcination technique which was postulated to strengthen grain bonding through the condensation of terminal silanol groups (Si-OH) present in zeolite grains. A substantial improvement in *p*-/*o*-xylene isomer separation was realized for RTP-treated columnar *c*-oriented MFI membranes grown on porous α-alumina discs and stainless steel tubes.[22] However, because the membranes were several micrometers thick, a second (conventional or RTP) calcination step was necessary to completely eliminate SDAs.

Here, we report the facile fabrication of zeolite membranes exhibiting high flux and high separation efficiency, using zeolite nanocrystal seed particles with well-controlled morphology obtained by confined synthesis (Scheme 1). Polycrystalline spherical aggregates (ca. 300 nm in diameter, Supporting Information, Figure S1) of zeolite seeds were directly deposited on home-made porous α-alumina supports using a rubbing method.[23] The seed particles were broken down into smaller grains (50–100 nm in diameter) and deposited in the pores of the support by the applied rubbing process. Subsequently, unbroken polycrystalline aggregates remaining on the support were pushed down deeper into the pores of the support or broken down further by a leveling process. This seed-deposition process could be completed in approximately one minute compared to conventional multi-step seeding methods that usually require several hours.

[*] W. C. Yoo, Prof. A. Stein
Department of Chemistry, University of Minnesota
Minneapolis, MN 55455 (USA)
Fax: (+1) 612-626-7541
E-mail: a-stein@umn.edu
Homepage: http://www.chem.umn.edu/groups/stein
J. A. Stoeger, P.-S. Lee, Prof. M. Tsapatsis
Department of Chemical Engineering & Materials Science
University of Minnesota, Minneapolis, MN 55455 (USA)

[**] Funding was provided by the NSF (mainly by CMMI-0707610 and in parts by DMR-0704312, DMR-0212302 and CBET-0522518). Parts of this work were carried out in the Institute of Technology Characterization Facility, University of Minnesota, which receives partial support from the NSF through the NNIN program and has received capital equipment funding from the NSF through the MRSEC, ERC, and MRI programs. The authors thank Prof. K. B. Yoon (Sogang University, Seoul, Korea) for valuable input regarding the implementation of the rubbing method.

Supporting information for this article is available on the WWW under http://dx.doi.org/10.1002/anie.201004029.

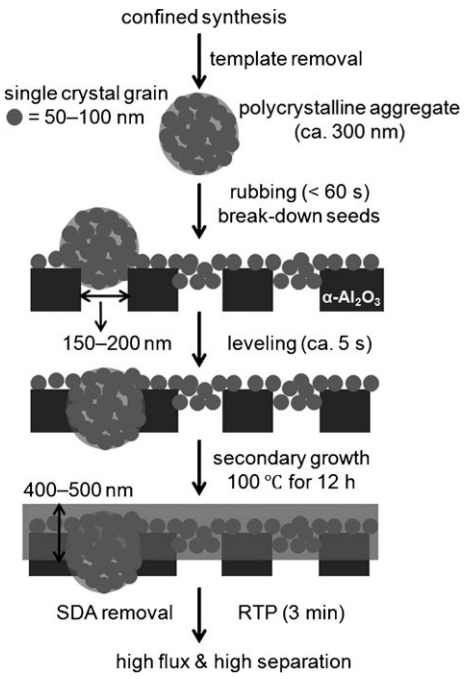

Scheme 1. Fabricating the high-performance zeolite membrane. Polycrystalline spherical aggregates of silicalite-1 (300 nm in diameter) were prepared by confined synthesis in 3DOM carbon.[8] These aggregates were broken down into single crystal grains (50–100 nm) by rubbing them directly onto a home-made α-alumina support to form a seed layer. Any remaining aggregates were either pushed down deeper into pores of the support or broken down further by a leveling process. The high-quality seed layer was used to prepare well-intergrown and very thin (400–500 nm) zeolite membranes with appropriate secondary growth conditions. The thin zeolite membranes were thermally treated to remove SDA molecules by conventional calcination (CC) or a rapid thermal processing (RTP) step.

Starting with the resulting high-quality seed layer, thin zeolite membranes (400–500 nm) were grown hydrothermally with good reproducibility. With such thin membranes, SDA removal to open the MFI pores was possible by a single RTP step that was completed in minutes, eliminating the need for slower and more energy-intensive, conventional calcination. As shown below, the RTP step also improved the performance of the zeolite membranes.

Confined syntheses have been of great interest for producing hierarchical zeolite catalysts and shape- and size-controlled seed particles for membrane applications,[7,8,24–31] Recently, three-dimensionally ordered macroporous (3DOM) carbon with interconnected pores was used to elucidate the mechanism of zeolite nanocrystal growth in confinement.[7,8] The growth patterns and the development of zeolite nanocrystal shapes could be controlled by altering the nutrient contents and the sequence of infiltration/hydrothermal (IHT) conditions. For example, growth-dominant conditions (high nutrient content) produced polycrystalline spherical aggregates ca. 300 nm in diameter composed of 50–100 nm grains after several IHT cycles. Due to the well-defined confining matrix, the molded polycrystalline aggregates are uniformly sized as indicated by their ability to form opaline arrays. In order to isolate the zeolite component after hydrothermal synthesis (Figure S1), the 3DOM carbon template was removed by calcination, which resulted in concurrent removal of the SDAs. For this step, oxidation of the 3DOM carbon–zeolite composite by treatment with nitric acid prior to calcination facilitated a more complete removal of the carbon phase, providing suitable seed particles for deposition on a porous support.

Yoon and co-workers reported that simply rubbing zeolite particles on large areas of smooth supports produced high-quality monolayers suitable as seed layers for membrane fabrication.[23] If the interaction between the support and an initial particle layer is stronger than the interaction between the first layer and subsequent layers, rubbing of the particles on the support removes excess material and yields a high-quality monolayer. Here we used this rubbing method to deposit the zeolite seed particles produced in the confined synthesis. To enhance the interaction between the first layer and the support, polyethyleneimine (PEI, 10 wt % in ethanol) was spin-coated on the α-alumina support (3000 rpm for 30 s) to provide a more hydrophilic surface. Polycrystalline aggregate spheres were directly rubbed on the α-alumina support. During rubbing, the polycrystalline aggregates broke down into individual silicalite-1 grains which entered the pores of the support as a consequence of the applied rubbing pressure (Figure 1 a). During this process the silicalite-1 structure was retained as illustrated in the XRD pattern of the seed layer in Figure S2. However, alteration of the surface structure cannot be excluded. The 50–100 nm-sized zeolite grains fit easily into the 150–200 nm pores at the top layer of the α-alumina support. Due to the sticky PEI layer and the tortuosity of the pores in the support, the seed particles did not enter deeper into the support (not shown here). A mesoporous silica interlayer, which was previously reported to smoothen the support for seed deposition,[5,6,9,12,16,17,22] was not needed.

While many of the polycrystalline sphere aggregates had broken up into individual grains after the rubbing procedure, numerous unbroken aggregates remained on the support (Figure 1 a and S3a). In order to obtain a more uniform seed layer, the remaining aggregates were pushed down deeper into the pores of the support by a separate leveling process, which could also break down the aggregates further. A gentle circular force was applied to the seed layer on a flat and rigid substrate, rendering the surface of the seed layer smoother in a time frame of less than 5 s (Figure 1 b and S3b). This simple leveling process successfully reduced the surface roughness and improved the uniformity of the membrane thickness.

Interstitial spaces between seeds were closed by immersing the coated membranes in a nutrient solution that promotes further zeolite growth during a secondary hydrothermal reaction. Preferential film orientations influence the permeation of molecules through the membrane and depend on the specific conditions of the hydrothermal reaction. The *c*-orientation is favored by high-temperature hydrothermal treatment (e.g., 175 °C), whereas *hoh*-out-of-plane orientations are preferentially obtained at lower temperatures (e.g., 100 °C).[16,17,32,33] Here we used lower temperature treatments at 100 °C for 12 h to minimize the zeolite film thickness. Figure 1 shows SEM images of samples obtained after secondary growth, starting with seed layers prepared by

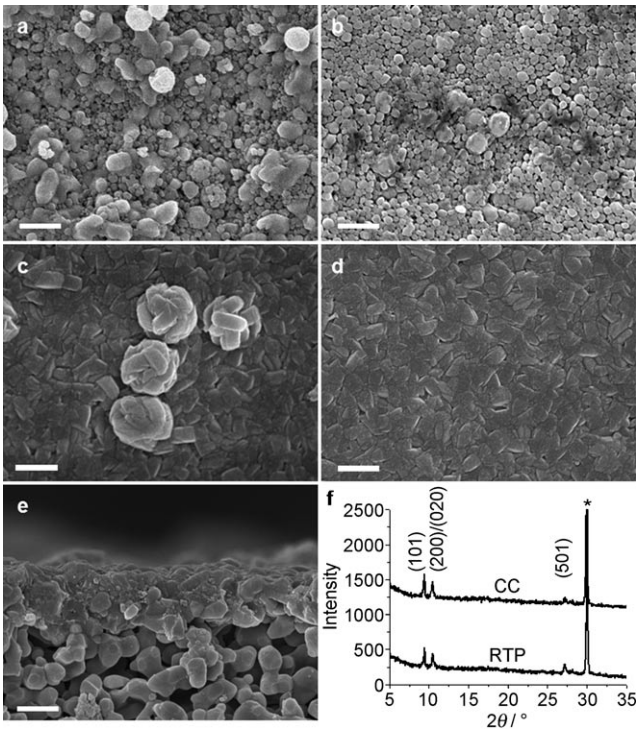

Figure 1. Development of the membrane. a–e) SEM images of seed layers and silicalite-1 seeded membranes on a porous α-alumina support at various stages of the fabrication process. a) Top view of a seed layer after the rubbing step and b) after rubbing and leveling. After secondary hydrothermal growth, intergrown MFI-zeolite layers are formed. c) In membranes prepared without leveling (denoted as R-membranes), several protrusions remain after secondary growth, but d) they are not prominent in membranes grown from the leveled seed layers shown in (b) (denoted as RL-membranes). e) The cross-sectional view of the RL-membrane after secondary growth shows an ultrathin MFI-zeolite layer on top of the α-alumina support. All scale bars correspond to 500 nm. f) X-ray diffraction patterns of zeolite films treated by conventional calcination (CC) and rapid thermal processing (RTP). The XRD patterns were acquired using a PANalytical X-Pert PRO MPD X-ray diffractometer equipped with a Co source ($Co_{K\alpha}$, $\lambda = 1.790$ Å) and an X-Celerator detector. The reflection peak marked with an asterisk (*) originates from the α-alumina support.

rubbing (denoted as R-membrane, panel c) or rubbing and leveling (denoted as RL-membrane, panel d). In both cases, fully intergrown zeolite films were generated after secondary growth, typically 400–500 nm thick (Figure 1e), which corresponds to some of the thinnest zeolite membranes reported so far.[20,21] The surface morphologies, however, differed for the two membranes. The R-membrane shows several surface protrusions in addition to a well-intergrown surface layer comprised of small grains several hundred nanometers in dimensions (Figure 1c and S3c). The protrusions originate from polycrystalline sphere aggregates that remained on the support after the rubbing procedure and grew only slightly bigger during secondary hydrothermal growth, from ca. 300 nm to ca. 500 nm. As indicated from permeation measurements (see below), the surface roughness in these zeolite films generated more stress-induced grain boundary defects during subsequent thermal treatment. On the other hand, SEM images of the RL-membrane prepared from the higher-quality seed layer reveal a more uniform surface, albeit with similar grain sizes as found in the R-membrane (Figure 1d and S3d).

Both types of membranes were thermally treated to remove SDAs by conventional calcination (CC, heated at 1 °C min^{-1} to 480 °C, held for 6 h and cooled at 1 °C min^{-1} to room temperature). The X-ray diffraction (XRD) patterns of the products revealed a characteristic MFI-type diffraction pattern, but there was no evidence for a preferred crystallographic orientation (Figure 1f). However, when the secondary growth time was extended, for example, to 20 h, keeping other conditions the same, patterns characteristic for preferred *hoh*-orientation appeared (Figure S4), consistent with previous reports involving secondary growth at relatively low temperatures (ca. 90–140 °C).[5,16,17,32,33] In addition, rapid thermal processing (RTP, heating at 700 °C min^{-1} to 700 °C and holding for 60 s) was evaluated as a method to remove SDA molecules occluded in the porous MFI crystals. In an initial report, RTP was considered as a pre-treatment step before conventional calcination in order to strengthen grain boundaries by condensation of terminal Si-OH groups located at the grain boundaries.[22] This pre-treatment changed the nature of defect/crack formation to lateral propagation instead of vertical propagation from the surface of the membrane to its support.[22] The MFI membranes studied by Choi et al. required a subsequent conventional or RTP calcination step to completely open the pore structure in RTP-treated zeolite membranes.[22] However, because the membranes described herein are an order of magnitude thinner, complete pore opening of the membranes was possible by using only one RTP treatment without any additional calcination. The XRD pattern of the product showed that membranes that had undergone only RTP treatment were structurally equivalent to those obtained by conventional calcination (Figure 1f).

To evaluate the membrane quality, permeation measurements involving the separation of *p*-xylene/*o*-xylene isomers were conducted. These measurements are based on the intrinsic capability of zeolite membranes for size-selective molecular separations. Separation factors (SF) improved significantly if a leveling step was employed during the membrane fabrication and if SDAs were removed by RTP rather than conventional calcination. As shown in Figure 1d and S3d, leveling leads to smoother seed layers, which favor the formation of smoother, highly intergrown films, while in the absence of leveling, overgrowths, like the ones shown in Figure 1c and S3c, are common. Such overgrowths have been associated with poor separation performance in the past, either because of poor intergrowth or due to stress-induced defects formed during calcination.[34] RTP-treated R-membranes exhibited increased separation factors (ca. 17) compared to ca. 8 for CC-treated R-membranes (Figure 2a and b). Furthermore, RTP-treated RL-membranes exhibited separation factors in the range from 123 to 139 and in one case as high as 335, compared to CC-treated RL-membranes with SF values of ca. 28 (Figure 2c and d). Separation factors of more than 100 for the separation of *p*-/*o*-xylene isomers have rarely been reported for such thin films.[19–21,35] In addition, all membranes generally permitted very high fluxes

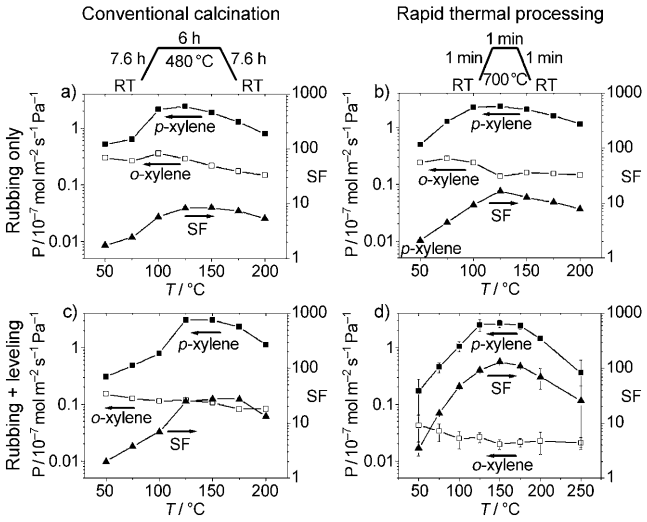

Figure 2. Permeation data and *p*-/*o*-xylene separation factors for nanocrystal-seeded membranes thermally treated by conventional calcination or rapid thermal processing (P = permeance, SF = separation factor). Graphs (a) and (b) correspond to R-membranes prepared without a leveling step and thermally treated by CC and RTP, respectively. Graphs (c) and (d) correspond to RL-membranes from preparations in which a leveling step was used and membranes were thermally treated by CC and RTP, respectively. Data points and error bars in (d) correspond to the three RL-membranes with separation factors in the range from 123 to 139.

of *p*-xylene due to the reduced membrane thickness. For example, the permeation flux of *p*-xylene through RTP-treated RL-membranes was ca. $2.6\times10^{-7}\,mol\,m^{-2}\,s^{-1}\,Pa^{-1}$ (Figure 2d), with a limiting permeation flux of ca. $4.0\times10^{-7}\,mol\,m^{-2}\,s^{-1}\,Pa^{-1}$ imposed by the home-made α-alumina support. Among zeolite membranes with SF values higher than 100, a permeation flux of *p*-xylene as high as $2.6\times10^{-7}\,mol\,m^{-2}\,s^{-1}\,Pa^{-1}$ is rarely achieved (Table 1). Although these data indicate a high-quality membrane and the absence of significant contributions to permeation by defects, there are still issues regarding the practical use of such membranes at the industrially relevant high pressure of xylenes and high temperatures, as indicated by the findings of Hedlund et al.[21]

Our study demonstrated that brittle, polycrystalline zeolite particles prepared by confined growth can produce seeds with suitable morphology for direct deposition onto a porous support by rubbing and leveling methods. Even though the resulting high-quality seed layers are initially randomly oriented, they can be converted to very thin (400–500 nm), well-intergrown zeolite films that exhibit high flux and excellent xylene isomer separation. Using an RTP step not only shortened the processing time and reduced energy usage, but also improved the membrane performance. Although the separation performance values of the reported membranes are not too different from the *b* oriented membranes of Ref. [5], the synthesis procedure reported here may be more attractive because it does not require the use of specially designed SDAs. The fact that seed layer formation and calcination steps could be completed in only a few minutes, significantly shortened the overall membrane fabrication process compared to conventional methods that involve complementary interactions between support and seed particles as well as slow calcination.[22] Similar processes of optimizing the deposition and calcination steps to obtain high flux membranes with high separation should be applicable to the nanofabrication of thin films with other compositions.

Table 1: Comparison of xylene isomer separation factors, permeation data and membrane structure for MFI-zeolite membranes from the present work and from select references.

	Calcination type	SF[c]	Permeance [10^{-7} mol m^{-2} s^{-1} Pa^{-1}]	Thickness [μm]	Orientation	*T* [°C][d]
R-membrane[a]	CC	ca. 8	ca. 2.0	0.4–0.5	random/*hoh*	150
	RTP	ca. 17	ca. 2.4	0.4–0.5	random/*hoh*	125
RL-membrane[b]	CC	ca. 28	ca. 3.0	0.4–0.5	random/*hoh*	150–175
	RTP	123–139, 335	2.6 ± 0.4	0.4–0.5	random/*hoh*	150
Ref. [22]	RTP + CC	126	0.48	ca. 10	*c*	125
Ref. [5]	CC	483	1.96	2	*b*	200
Ref. [21]	CC	3	6.0	0.5	random	100

[a] Membranes denoted as R-membrane were fabricated using a seed layer deposited on the α-alumina support by the rubbing method. [b] Membranes denoted as RL-membrane were fabricated using a seed layer deposited on the α-alumina support by the rubbing and leveling methods. 123–139 is the range found for three membranes and 335 is the value for the highest performing membrane that was synthesized, all using the same conditions. Data for individual RTP-treated RL-membranes are provided in Figure S5. [c] The separation factor (SF) is defined as the ratio of the permeances of *p*-xylene/*o*-xylene that passed through the membrane. [d] This temperature corresponds to the temperature at which the highest separation factor was obtained (SF value shown).

Received: July 1, 2010
Revised: August 27, 2010
Published online: September 30, 2010

Keywords: hydrothermal synthesis · separation · thin films · zeolite membranes · zeolites

[1] M. E. Davis, *Nature* **2002**, *417*, 813.
[2] J. Caro, M. Noack, *Microporous Mesoporous Mater.* **2008**, *115*, 215.
[3] E. E. McLeary, J. C. Jansen, F. Kapteijn, *Microporous Mesoporous Mater.* **2006**, *90*, 198.
[4] J. Coronas, *Chem. Eng. J.* **2010**, *156*, 236.
[5] Z. Lai, G. Bonilla, I. Diaz, J. G. Nery, K. Sujaoti, M. A. Amat, E. Kokkoli, O. Terasaki, R. W. Thompson, M. Tsapatsis, D. G. Vlachos, *Science* **2003**, *300*, 456.
[6] M. A. Snyder, M. Tsapatsis, *Angew. Chem.* **2007**, *119*, 7704; *Angew. Chem. Int. Ed.* **2007**, *46*, 7560.
[7] W. C. Yoo, S. Kumar, R. L. Penn, M. Tsapatsis, A. Stein, *J. Am. Chem. Soc.* **2009**, *131*, 12377.
[8] W. C. Yoo, S. Kumar, Z. Wang, N. S. Ergang, W. Fan, G. N. Karanikolos, A. V. McCormick, R. L. Penn, M. Tsapatsis, A. Stein, *Angew. Chem.* **2008**, *120*, 9236; *Angew. Chem. Int. Ed.* **2008**, *47*, 9096.
[9] J. Choi, S. Ghosh, L. King, M. Tsapatsis, *Adsorption* **2006**, *12*, 339.

[10] J. S. Lee, Y.-J. Lee, E. L. Tae, Y. S. Park, K. B. Yoon, *Science* **2003**, *301*, 818.
[11] K. B. Yoon, *Acc. Chem. Res.* **2007**, *40*, 29.
[12] J. Choi, S. Ghosh, Z. Lai, M. Tsapatsis, *Angew. Chem.* **2006**, *118*, 1172; *Angew. Chem. Int. Ed.* **2006**, *45*, 1154.
[13] Y. Liu, Y. Li, W. Yang, *Chem. Commun.* **2009**, 1520.
[14] Y. Liu, Y. Li, W. Yang, *J. Am. Chem. Soc.* **2010**, *132*, 1768.
[15] I. Lee, J. L. Buday, H.-K. Jeong, *Microporous Mesoporous Mater.* **2009**, *122*, 288.
[16] A. Gouzinis, M. Tsapatsis, *Chem. Mater.* **1998**, *10*, 2497.
[17] G. Xomeritakis, Z. Lai, M. Tsapatsis, *Ind. Eng. Chem. Res.* **2001**, *40*, 544.
[18] C. J. Gump, V. A. Tuan, R. D. Noble, J. L. Falconer, *Ind. Eng. Chem. Res.* **2001**, *40*, 565.
[19] W. Yuan, Y. S. Lin, W. Yang, *J. Am. Chem. Soc.* **2004**, *126*, 4776.
[20] J. Hedlund, F. Jareman, A.-J. Bons, M. Anthonis, *J. Membr. Sci.* **2003**, *222*, 163.
[21] J. Hedlund, J. Sterte, M. Anthonis, A.-J. Bons, B. Carstensen, N. Corcoran, D. Cox, H. Deckman, W. D. Gijnst, P.-P. d. Moor, F. Lai, J. McHenry, W. Mortier, J. Reinoso, J. Peters, *Microporous Mesoporous Mater.* **2002**, *52*, 179.
[22] J. Choi, H.-K. Jeong, M. A. Snyder, J. A. Stoeger, R. I. Masel, M. Tsapatsis, *Science* **2009**, *325*, 590.
[23] J. S. Lee, J. H. Kim, Y. J. Lee, N. C. Jeong, K. B. Yoon, *Angew. Chem.* **2007**, *119*, 3147; *Angew. Chem. Int. Ed.* **2007**, *46*, 3087.
[24] W. Fan, M. A. Snyder, S. Kumar, P.-S. Lee, W. C. Yoo, A. V. McCormick, R. L. Penn, A. Stein, M. Tsapatsis, *Nat. Mater.* **2008**, *7*, 984.
[25] B. T. Holland, L. Abrams, A. Stein, *J. Am. Chem. Soc.* **1999**, *121*, 4308.
[26] C. J. H. Jacobsen, C. Madsen, T. V. W. Janssens, H. J. Jakobsen, J. Skibsted, *Microporous Mesoporous Mater.* **2000**, *39*, 393.
[27] S.-S. Kim, J. Shah, T. J. Pinnavaia, *Chem. Mater.* **2003**, *15*, 1664.
[28] C. Madsen, C. J. H. Jacobsen, *Chem. Commun.* **1999**, 673.
[29] I. Schmidt, C. Madsen, C. J. H. Jacobsen, *Inorg. Chem.* **2000**, *39*, 2279.
[30] L. Tosheva, V. P. Valtchev, *Chem. Mater.* **2005**, *17*, 2494.
[31] J. Wang, A. Vinu, M.-O. Coppens, *J. Mater. Chem.* **2007**, *17*, 4265.
[32] G. Bonilla, D. G. Vlachos, M. Tsapatsis, *Microporous Mesoporous Mater.* **2001**, *42*, 191.
[33] A.-J. Bons, P. D. Bons, *Microporous Mesoporous Mater.* **2003**, *62*, 9.
[34] G. Xomeritakis, A. Gouzinis, S. Nair, T. Okubo, M. He, R. M. Overney, M. Tsapatsis, *Chem. Eng. Sci.* **1999**, *54*, 3521.
[35] S. Miachon, P. Ciavarella, L. van Dyk, I. Kumakiri, K. Fiaty, Y. Schuurman, J.-A. Dalmon, *J. Membr. Sci.* **2007**, *298*, 71.

